Journal of Electroceramics
https://doi.org/10.1007/s10832-018-0113-6

Effect of Ca substitution on microwave dielectric properties of BaV_2O_6 ceramics

Guoguang Yao[1,2] · Zhaoyu Ren[1] · Peng Liu[3]

Received: 27 November 2016 / Accepted: 22 January 2018

Abstract
Effects of Ca substitution for Ba on the phase composition, microstructure, sintering behavior and microwave dielectric properties of nominal ceramics $Ba_{1-x}Ca_xV_2O_6$ ($0.2 \le x \le 0.5$) were investigated. The XRD, Raman and SEM results revealed that BaV_2O_6 and CaV_2O_6 composite ceramics were formed. Nominal ceramics $Ba_{1-x}Ca_xV_2O_6$ could be well densified at about 550 °C via a solid-state reaction method. The microwave dielectric properties exhibited strong dependence on the composition and microstructure. Typically, the $Ba_{0.7}Ca_{0.3}V_2O_6$ ceramics sintered at 550 °C exhibited excellent microwave dielectric properties: $\varepsilon_r = 10.9$, Qxf = 17,100 GHz (at 9.9 GHz), and $\tau_f = 4$ ppm/°C. Meanwhile, $Ba_{0.7}Ca_{0.3}V_2O_6$ ceramics also showed good chemical compatibility with Al electrode. These results indicated that the $Ba_{0.7}Ca_{0.3}V_2O_6$ ceramics could be a promising candidate for the ULTCC technology.

Keywords Sintering · Crystal structure · Dielectric properties

1 Introduction

In recent years, enormous research has been devoted to developing microwave dielectric ceramics with low permittivity ($\varepsilon_r < 15$), high quality factor ($Q \times f$), and a near-zero temperature coefficient of resonant frequency (τ_f), which are widely used for substrate, radar for Pre-Crash Safety System, and noncompressed digital video transmission system, etc. [1–3]. Besides, during the past three decades, low temperature co-fired ceramic (LTCC) technology has been developed to accommodate the requirements of high-stability, low-cost and miniaturization for the microwave devices. This LTCC technology is used to fabricate three-dimensional ceramic modules with low dielectric loss and embedded silver electrode [4–6]. Moreover, the latest trend in LTCC technology is to develop new dielectrics with ultra-low sintering temperature (Ts < 660 °C) to save energy, protect environment, and to enable further seamless integration with silicon technology, metals or even organic substrates [7, 8]. The continuous efforts in this facet have resulted in a new class of materials known as ultra-low-temperature co-fired ceramics (ULTCC), wherein the base ceramic composition sinters at temperatures lower than the melting point of aluminum electrode (660 °C) [9, 10].

Recently extensive efforts have been made in vanadate compounds to identify novel microwave ceramic systems suitable for application in LTCC substrate since they possess low or even ultra-low sintering temperature and excellent microwave dielectric properties [11–15]. In BaO-V_2O_5 binary system, five phases are formed: $Ba_3(VO_4)_2$, $Ba_2V_2O_7$, $Ba_3V_4O_{13}$, $Ba_{16}V_{18}O_{61}$ and BaV_2O_6 [16–20]. All of them show good microwave dielectric properties ($\varepsilon_r = 9.6$~17, $Q \times f = 21{,}800$~$80{,}100$ GHz and $\tau_f = -64$~40 ppm/°C) and inherently low or ultra-low sintering temperature, except for $Ba_3(VO_4)_2$ (Ts = 1600 °C). In particular, the orthorhombic structure BaV_2O_6 ceramic is of special interest due to its exceptionally relatively low ε_r but a large positive τ_f value (40 ppm/°C) [21], which can be used as a novel temperature compensator. However, any practical application of this material in ULTCC technology has been restricted because its large positive τ_f. An easy and effective approach to compensate τ_f through zero is to combine two chemical compounds with τ_f of opposite signs to form a solid solution or composite

✉ Guoguang Yao
yaoguoguang@xupt.edu.cn

[1] Institute of Photonics & Photon-Technology, Northwest University, Xi'an 710069, China

[2] School of Science, Xi'an University of Posts and Telecommunications, Xi'an 710121, China

[3] College of Physics and Information Technology, Shaanxi Normal University, Xi'an 710062, China

Published online: 06 February 2018

materials [22]. Especially for diphasic ceramics with different crystal structures, it has been proved to be effectively inhibited the formation of the solid solutions or secondary phases, and guaranteed the desirable microwave dielectric properties [23]. Recently, we have reported the monoclinic structure CaV_2O_6 ceramic sintered at 675 °C, which exhibited a high Qxf of 123,000 GHz and a large negative τ_f of −60 ppm/°C [24], compared to BaV_2O_6 ceramic (Qxf = 21,800 GHz, τ_f = 40 ppm/ °C) [18, 21]. Thus, a near-zero τ_f may be obtained by preparing $Ba_{1-x}Ca_xV_2O_6$ ceramics. It was shown that the tuning of the phase formation, and therefore the final functional properties, was the result of a simple optimization of the sintering and the $Ba_{1-x}Ca_xV_2O_6$ compositional parameters. Dense, nominal ceramics $Ba_{1-x}Ca_xV_2O_6$ were prepared and a detailed investigation was performed to provide an insight into the relations between the structure and the microwave dielectric properties.

2 Experimental procedure

The starting materials are high-purity oxide powders or carbonates powders (>99.9%; Guo-Yao Co. Ltd., Shanghai, China): $BaCO_3$, $CaCO_3$, and V_2O_5. Predried raw materials were separately weighed in stoichiometric mixtures $Ba_{1-x}Ca_xV_2O_6$ ($0.2 \le x \le 0.5$) and ball-milled for 8 h in a nylon jar with agate balls and ethanol as media. The resultant slurry was dried, then ground well, and calcined at 500 °C for 3 h. The calcined powders were reground for 8 h, dried, mixed with 5 wt% polyvinyl alcohol (PVA) as a binder, and granulated. The granulated powders were uniaxially pressed into pellets 10 mm in diameter and 5 mm in thickness under a pressure of 100 MPa. These pellets were sintered from 525 to 600 °C for 4 h in air with a heating rate of 5 °C/min, and then cooled to room temperature.

The bulk densities of the sintered ceramics were measured by Archimedes' method. The crystal structures were analyzed using powder X-ray diffraction (XRD) with Cu Ka radiation (Rigaku D/MAX2550, Tokyo, Japan). The Raman spectra were collected at room temperature using a Raman Microscope (Horiba Jobin Yvon S.A.S., France) with Ar ion laser (514 nm) operated at 30 mw. The microstructure of pellets was investigated using a scanning electron microscope (SEM, Fei Quanta 200, Eindhoven, Holland) coupled with energy dispersive X-ray spectroscopy (EDS). The microwave dielectric properties of sintered samples were measured using a network analyzer (ZVB20, Rohde&schwarz, Munich, Germany) with the $TE_{01\delta}$ shielded cavity method. The temperature coefficient of resonant frequency (τ_f) was calculated with the following Eq. (1):

$$\tau_f = \frac{f_{80} - f_{20}}{f_{20} \times (80-20)} \quad (1)$$

where f_{80} and f_{20} are the resonant frequency at 80 °C and 20 °C, respectively.

3 Results and discussion

Figure 1 shows the XRD patterns of $Ba_{1-x}Ca_xV_2O_6$ ceramics fired at 550 °C for 4 h. All the peaks could be well indexed by BaV_2O_6 (JCPDS #34–0014) and CaV_2O_6 (JCPDS #29–0211) phases and no secondary phase was detected, indicating that a stable composite system BaV_2O_6-CaV_2O_6 was formed. Moreover, the intensity of the diffraction peaks of BaV_2O_6 phase decreased and CaV_2O_6 phase increased gradually, as the amount of x increased. Furthermore, as shown in Fig. 1, the main peak (131) of BaV_2O_6 shifted toward to high angle with increasing Ca concentration, suggesting that partial substitution of Ba^{2+} (C.N. = 12, 1.61 Å) by smaller ion

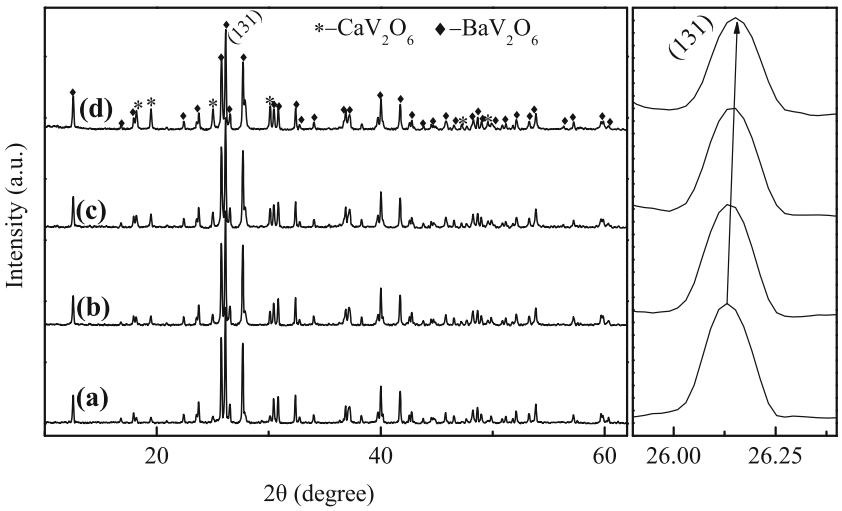

Fig. 1 XRD patterns of $Ba_{1-x}Ca_xV_2O_6$ ceramics fired at 550 °C for 4 h: (a) x = 0.2, (b) x = 0.3, (c) x = 0.4, (d) x = 0.5

Ca^{2+}(C.N. = 12, 1.34 Å) also occurred. The formed BaV_2O_6-CaV_2O_6 composite ceramics would be beneficial for the successful compensation of the dielectric properties of BaV_2O_6-host ceramic, especially for τ_f.

Microwave dielectric properties of $Ba_{1-x}Ca_xV_2O_6$ ceramics system sintered at 550 °C for 4 h are summarized in Table 1. As x increased from 0.2 to 0.5, the τ_f values decreased from 9.0 to −10.0 ppm/°C and a near-zero τ_f could be obtained for $Ba_{0.7}Ca_{0.3}V_2O_6$ specimen.

The XRD patterns of the $Ba_{0.7}Ca_{0.3}V_2O_6$ ceramics sintered at different temperatures are displayed in Fig. 2. No structural change and secondary phase were observed while increasing the sintering temperature from 525 to 600 °C. This means that the BaV_2O_6-CaV_2O_6 composite ceramics can coexist well in sintering temperature range of 525–600 °C.

Figure 3 displays the room temperature Raman spectra of $Ba_{1-x}Ca_xV_2O_6$ pellets. The spectra can be interpreted as a combination of the typical Raman spectra of the end members BaV_2O_6 and CaV_2O_6. The observed Raman bands and Raman band assignments for CaV_2O_6 are list in Table 2, according to previous report by Baran et al. [25]. Ten Raman bands are identified in the spectrum of pure phase BaV_2O_6, based on the previous Raman experiments of BaV_2O_6 [18, 26]. The Raman bands observed in the region 875–965 cm^{-1} can be identified as the symmetric stretching vibrations of $(VO_4)^{3-}$ anions. The asymmetric bending vibration of $(VO_4)^{3-}$ are observed at 818 and 523 cm^{-1}, whereas the symmetric bending vibrations occurs at 402 and 468 cm^{-1}. The Raman bands observed below 400 cm^{-1} can be assigned to VO_2 rocking, twisting, and chain deformation vibrations. Moreover, the Raman modes in BaV_2O_6 decreased strongly in intensity with increasing Ca content in nominal ceramic $Ba_{1-x}Ca_xV_2O_6$. Thus, the mixture phase formation of BaV_2O_6-CaV_2O_6 was further verified in the Raman spectra on the decline of certain modes.

Figure 4 illustrates SEM surface micrographs and EDS spectra of the $Ba_{0.7}Ca_{0.3}V_2O_6$ ceramics sintered at different temperatures. A porous microstructure was developed in the pellets sintered at 525 °C, and a relative homogeneous and compact microstructure with less porosity was achieved for sample fired at 550 °C. However, when the sintering temperature exceeded 550 °C, the abnormal grain growth and partial grain melting appeared, as seen in Figs. 4(c), (d). In addition,

Table 1 Microwave dielectric properties of $Ba_{1-x}Ca_xV_2O_6$ ceramics sintered at 550 °C for 4 h

Compounds	density (g/cm^3)	ε_r	Qxf (GHz)	τ_f (ppm/°C)
$Ba_{0.8}Ca_{0.2}V_2O_6$	2.981	9.4	10,000	9.0
$Ba_{0.7}Ca_{0.3}V_2O_6$	3.559	10.9	17,100	4.0
$Ba_{0.6}Ca_{0.4}V_2O_6$	3.315	9.0	14,400	−6.0
$Ba_{0.5}Ca_{0.5}V_2O_6$	3.212	8.3	13,400	−10.0

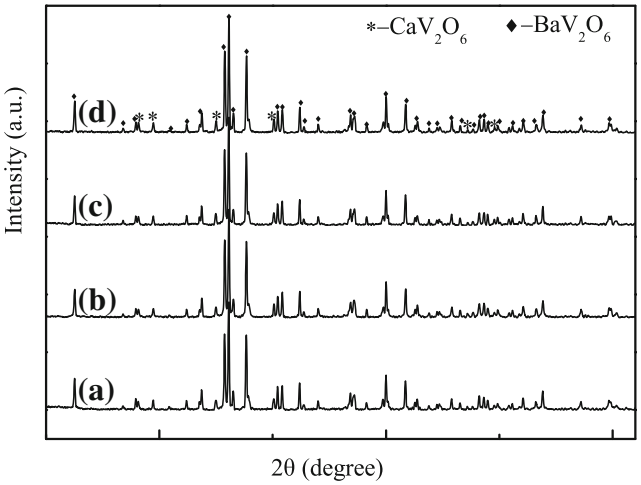

Fig. 2 XRD patterns of the $Ba_{0.7}Ca_{0.3}V_2O_6$ ceramics sintered at different temperatures: (a) 525 °C, (b) 550 °C, (c) 575 °C, (d) 600 °C

the coexistence of two different colors grains were observed, as marked in Fig. 4(b).Therefore, EDS analysis was conducted to distinguish the compositional difference between them and the corresponding results are shown in Fig. 4(e), (f). It can be clearly seen that the light-colored grains (Spot A) mainly contained Ba, V and O and a little amount of Ca elements, whereas the dim grains (Spot B) were dominantly composed of Ca, V and O and a small amount of Ba elements. Comparing these results with XRD analysis and Raman spectra, it can be confirmed that the light-colored grains are identified as BaV_2O_6 phase, and the dim grains are identified as CaV_2O_6 phase. Meanwhile, a slight ionic diffusion between BaV_2O_6 and CaV_2O_6 phases also occurred, which would deteriorate the microwave dielectric properties of composite ceramics.

Figure 5 presents the density and microwave dielectric properties of the $Ba_{0.7}Ca_{0.3}V_2O_6$ ceramics as a function of sintering temperature. As shown in Fig. 5(a), with an

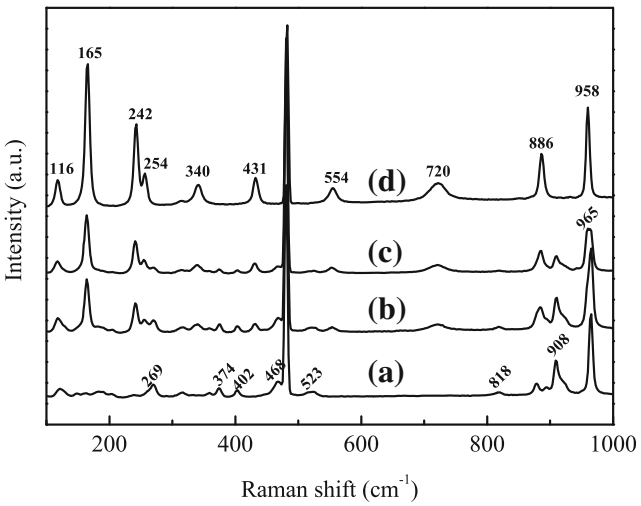

Fig. 3 Room temperature Raman spectra of $Ba_{1-x}Ca_xV_2O_6$ ceramics: (a) x = 0.0, (b) x = 0.3, (c) x = 0.5, (d) x = 1.0.

Table 2 Observed Raman frequencies (cm^{-1}) and band assignments for CaV_2O_6 at room temperature

Raman frequency	Assignment[a]
958	$\nu(VO)^{str}$
886	$\nu^{as}(VOV)$
720 554}	$\nu(V_2O_2)_n + \nu(VO_3)^{str}$
431	$\nu^{s}(VOV)^{str}$
340 254}	CaO_6 modes
242	lattice modes
165 116}	$\nu(V_2O_2)_n$

[a] *str* stretch, *as* antisymmetric stretch, *s* symmetric stretch

increment of sintering temperature, the bulk density of specimens increased to maximum values, corresponding to the optimal densification temperature, and declined thereafter. The initial enhancement in density with increasing sintering temperature was associated with the grain growth and the subsequent removal of porosity, whereas the deterioration in density at temperatures above 550 °C was due to the abnormal grain growth as well as partial grain melting (seen Fig. 4(e), (f)). As expected, the relationship between the ε_r and the sintering temperature showed the same trend as that of bulk density vs sintering temperature. A maximum ε_r value ~10.9 was obtained at the optimum densification temperature of 550 °C. As seen in Fig. 5(b), when the sintering temperature increased from 525 to 550 °C, the Qxf value increased from 11,500 to the peak value of 17,100 GHz, and then it gradually decreased with further increasing sintering temperature. The ε_r and Qxf values of ceramics are influenced much by many of the same reasons, including ionic polarizability, bulk density, microstructure, lattice defects, and grain sizes etc. [27, 28]. In the present research, high densification and homogeneous microstructure resulted in a large ε_r and a high Qxf value. In addition, the optimum Qxf value of 17,100 GHz for $Ba_{0.7}Ca_{0.3}V_2O_6$ composite ceramic is somewhat lower than that of BaV_2O_6 (Qxf=21,800 GHz) [21], but much lower than that of CaV_2O_6 (Qxf=123,000 GHz) [24]. The reason may be due to the factor that the microwave dielectric properties of each phase may be different in composite ceramics from those in the monophasic ceramics owing to the diffusion of different

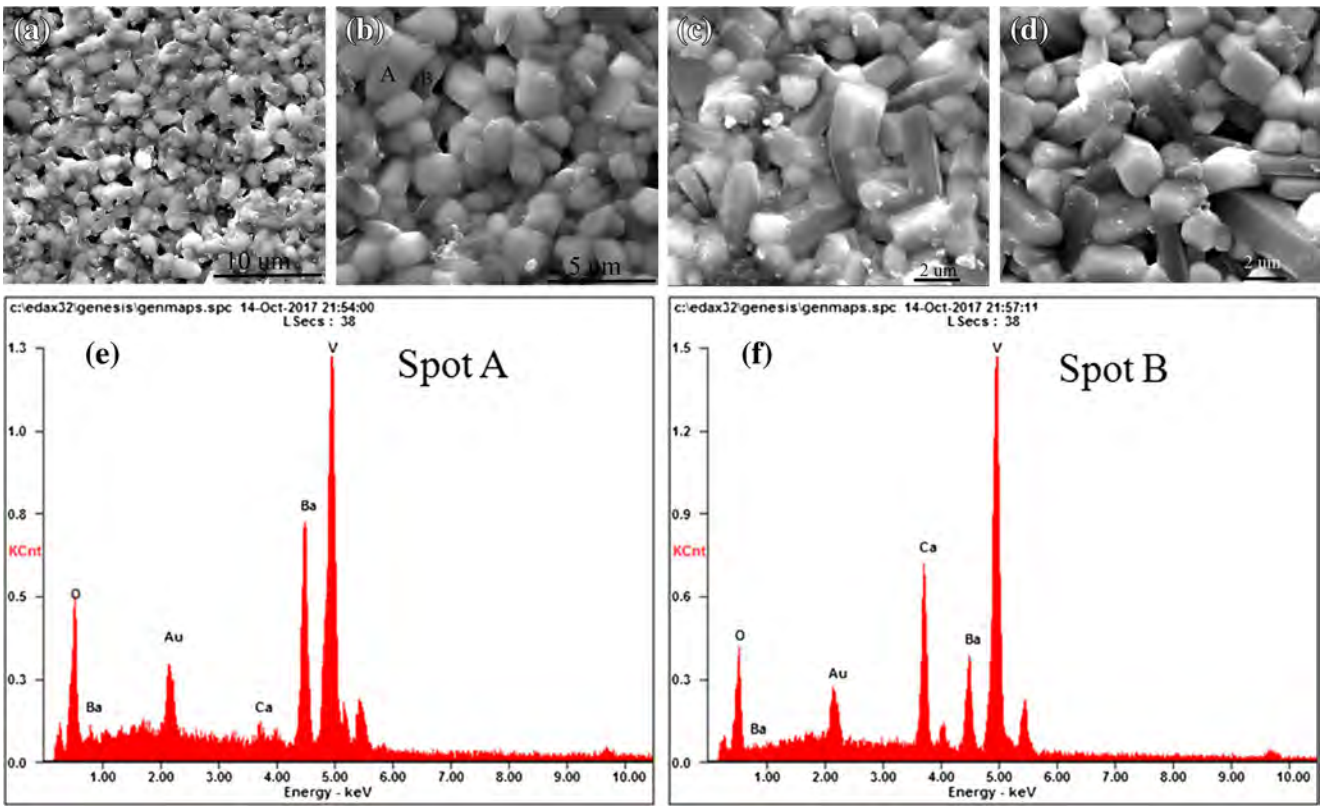

Fig. 4 SEM micrographs and EDS spectra of the $Ba_{0.7}Ca_{0.3}V_2O_6$ ceramics sintered at different temperatures: (**a**) 525 °C, (**b**) 550 °C, (**c**) 575 °C, (**d**) 600 °C, and (**e**) and (**f**) EDS spectra corresponding to (**b**)

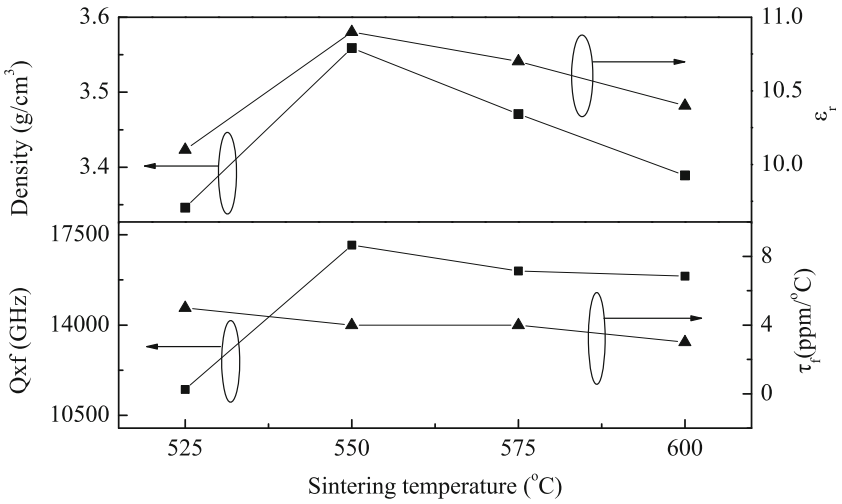

Fig. 5 (a) Density and ε_r and (b) Qxf and τ_f of the $Ba_{0.7}Ca_{0.3}V_2O_6$ ceramics as a function of sintering temperature

ions (seen in Figs. 1 and 4(e), (f)), as well as their difference in microstructure (grain orientation, the average grain size, phase distribution) [21, 24, 29]. As for the τ_f value, a near zero τ_f value about 4.0 ppm/°C was obtained, and it was almost temperature independent in the range of 525–600 °C. This is expected because there is no structural and compositional variation involved [30].

The chemical compatibility of ULTCC material with aluminum is of major concern for practical applications. Therefore, it is necessary to study whether the aluminum reacts with the $Ba_{0.7}Ca_{0.3}V_2O_6$ ceramic or not. Figure 6 illustrates the XRD pattern, SEM image and EDS analysis of the $Ba_{0.7}Ca_{0.3}V_2O_6$ ceramics after cofired with 20 wt% Al powders at 550 C for 4 h. As shown in Fig. 6, only peaks of Al, BaV_2O_6, and CaV_2O_6 phases could be separately identified and no additional peaks were developed. Meanwhile, as seen in the inset of Fig. 6, a reaction-free and good contact between the $Ba_{0.7}Ca_{0.3}V_2O_6$ ceramics and Al were observed from the SEM image. Both the XRD and SEM-EDS analysis results confirmed that the $Ba_{0.7}Ca_{0.3}V_2O_6$ ceramics did not react with Al at the sintering temperature. Comparison of our proposed dielectrics with some V-based ceramics is made, as summarized in Table 3. As seen in Table 3, the large negative or positive τ_f value is a common feature for other relative ceramics compared to our present work, which inhibit their further applications to a large extent. Conversely, our $Ba_{0.7}Ca_{0.3}V_2O_6$ ceramics possessed a near zero τ_f, available microwave dielectric properties ($\varepsilon_r = 10.9$, Qxf = 17,100 GHz), and ultra-low sintering temperature. These merits make it a more attractive material for ULTCC applications.

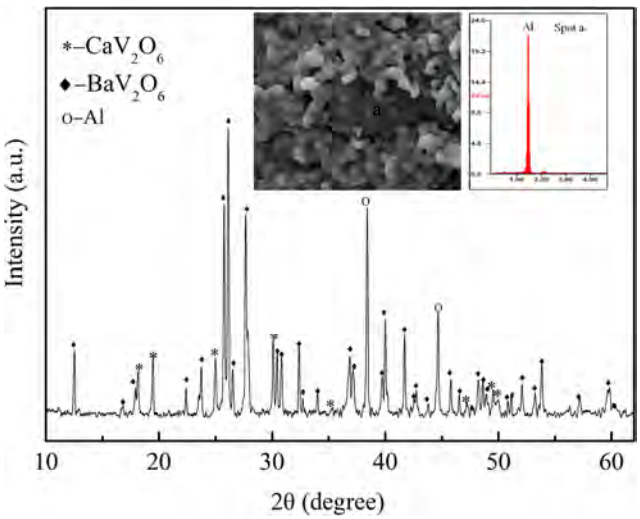

Fig. 6 XRD pattern, SEM image and EDS analysis of the $Ba_{0.7}Ca_{0.3}V_2O_6$ ceramics after cofired with 20 wt% Al powders at 550 C for 4 h

4 Conclusions

Temperature stable $Ba_{1-x}Ca_xV_2O_6$ ceramics were successfully manufactured by a conventional solid-state reaction route. The phase constitution, microstructure, compatibility with aluminum, and microwave dielectric properties were investigated. The ultra-low-temperature sinterability and

Table 3 Comparison of the proposed dielectrics with some V-based ceramics

Compounds	ε_r	Qxf (GHz)	τ_f (ppm/°C)	ST (°C)	Ref.
$Ba_{0.7}Ca_{0.3}V_2O_6$	10.9	17,100	4.0	550	*
$Ba_3V_4O_{13}$	9.6	56,000	−42.0	600	[16]
$Ba_{16}V_{18}O_{61}$	9.7	80,100	−64.0	620	[17]
BaV_2O_6	11.2	42,800	28.0	550	[18]
CaV_2O_6	10.2	123,300	−60.0	800	[23]
$BaZnV_2O_7$	10.7	31,000	−64.0	720	[31]
$Ba_5V_4O_{15}$	12.1	26,790	7.0	900	[32]

*this work

desirable microwave dielectric properties can be obtained by adjusting the ration of Ba/Ca at a suitable value in $Ba_{1-x}Ca_xV_2O_6$ systems. Typically, the dense $Ba_{0.7}Ca_{0.3}V_2O_6$ composite ceramics sintered at 550 °C for 4 h exhibited excellent microwave dielectric properties of $\varepsilon_r = 10.9$, Qxf = 17,100 GHz (at 9.9 GHz), and $\tau_f = 4$ ppm/°C, it also owned good chemical compatibility with Al electrode. These merits make it a promising material for ULTCC applications.

Acknowledgements This work is supported by the National Natural Science Foundation of China (Grants No. 51402235). China's Postdoctoral Science Fund (Grant No. 2015 M582696), and by Shaanxi Province Postdoctoral Science Foundation.

References

1. K.X. Song, P. Liu, H.X. Lin, W.T. Su, Z.H. Ying, J. Eur. Ceram. Soc. **36**, 1167 (2016)
2. J. Zhang, Y.Y. Zhou, B. Peng, Z.X. Yue, J. Am. Ceram. Soc. **97**, 3537 (2014)
3. W. Jin, W.L. Yin, S.Q. Yu, M.J. Tang, Mater. Lett. **173**, 47 (2016)
4. T.A. Vanderah, Science **298**, 1182 (2002)
5. M. Valant, D. Suvorov, J. Am. Ceram. Soc. **84**, 2900 (2001)
6. D. Zhou, L.X. Pang, Z.M. Qi, B.B. Jin, X. Yao, Sci. Rep-UK. **4**, 1 (2014)
7. R.R. Turnmala, J. Am. Ceram. Soc. **74**, 895 (1991)
8. H. Kahari, M. Teirikangas, H.L. Jantunen, J. Am. Ceram. Soc. **97**, 3537 (2014)
9. M.T. Sebastian, H. Wang, H.L. Jantunen, Curr. Opin. Solid State Mater. Sci. **20**, 151 (2016)
10. H.T. Yu, J.S. Liu, W.L. Zhang, S.R. Zhang, J. Mater, Sci. Mater. Electron. **26**, 9414 (2015)
11. E.K. Suresh, A.N. Unnimaya, A. Surjith, R. Ratheesh, Ceram. Int. **39**, 3635 (2013)
12. L. Fang, C.X. Su, H.F. Zhou, H. Zhang, J. Am. Ceram. Soc. **96**, 688 (2013)
13. C.H. Su, Y.S. Wang, C.L. Huang, J. Alloys. Compd. **641**, 93 (2015)
14. H.F. Zhou, F. He, X.L. Chen, L. Fang, J. Mater. Sci. Mater. Electron. 25, 1480 (2014)
15. G.G. Yao, P. Liu, J.J. Zhou, H.W. Zhang, J. Eur. Ceram. Soc. **34**, 2983 (2014)
16. S.E. Kalathil, A. Neelakantan, R. Ratheesh, J. Am. Ceram. Soc. **97**, 1530 (2014)
17. E.K. Suresh, K. Prasad, N.S. Arun, R. Ratheesh, J. Electron. Mater. **45**, 2996 (2016)
18. U.A. Neelakantan, S.E. Kalathil, R. Ratheesh, Eur. J. Inorg. Chem. **2**, 305 (2015)
19. R. Umemura, H. Ogawa, A. Yokoi, H. Ohsato, A. Kan, J. Alloys Compd. **424**, 388 (2006)
20. M.R. Joung, J.S. Kim, M.E. Song, S. Nahm, J. Am. Ceram. Soc. **92**, 3092 (2009)
21. C.J. Pei, G.G. Yao, Z.Y. Ren, J. Ceram. Process. Res. **17**, 681 (2016)
22. F.F. Gu, G.H. Chen, X.Q. Li, M. Li, Mater. Chem. Phys. **167**, 354 (2015)
23. P.L. Wise, I.M. Reaney, W.E. Lee, J. Mater. Res. **17**, 2033 (2002)
24. G.G. Yao, C.J. Pei, P. Liu, H.W. Zhang, J. Mater, Sci. Mater. Electron. **26**, 7719 (2015)
25. E.J. Baran, C.I. Cabello, A.G. Nord, J. Raman Spectrosc. **18**, 405 (1987)
26. Y. Li, R.L. Tang, N. Li, X.D. Zhao, P.W. Zhu, X. Wang, J. Appl. Phys. **118**, 035902 (2015)
27. S.J. Penn, N.M. Alford, A. Templeton, X. Wang, M. Xu, M. Reece, K. Schrapel, J. Am. Ceram. Soc. **80**, 1885 (1997)
28. N. Ichinose, T. Shimada, J. Eur. Ceram. Soc. **26**, 1755 (2006)
29. C. Zhang, R.Z. Zuo, J. Alloys Compd. **622**, 362 (2015)
30. S.D. Skapin, U. Pirnat, B. Jancar, D. Suvorov, J. Am. Ceram. Soc. **98**, 3818 (2015)
31. L. Fang, Z. Wei, C. Su, F. Xiang, H. Zhang, Ceram. Int. **40**, 16835 (2014)
32. A.N. Unnimaya, E.K. Suresh, J. Dhanya, R. Ratheesh, J. Mater, Sci. Mater. Electron. **25**, 1127 (2014)